Modified infiltration of solvated ions and ionic liquid in a nanoporous carbon

Weiyi Lu · Taewan Kim · Cang Zhao · Xi Chen · Yu Qiao

Abstract Infiltration of ions in a nanoporous carbon is responsive to the external electric field. If the liquid phase is an aqueous solution of electrolyte, the effective solid-liquid interfacial tension decreases as the voltage rises, similar to the electrowetting phenomenon at a large graphite surface. If the liquid phase is an ionic liquid, however, the effective interfacial tension increases with the voltage. The accessible nanopore volume is not dependent on the electric field. The unique phenomena should be related to the confinement effects of the nanopore inner surfaces.

1 Introduction

Liquids confined in nanoenvironment are fundamentally different from their bulk counterparts [1]. Immediately next to a nanochannel inner surface, the water molecular density can be either higher or lower than the average level, depending on the nature of the solid-liquid interaction [2]. Beyond the interface layer, the molecular distribution along the radius direction can be layered, and the layered structure would be different if the environmental factors, such as temperature, pressure gradient, and electric field, vary [3–5].

W. Lu · C. Zhao · Y. Qiao (✉)
Department of Structural Engineering, University of California—San Diego, La Jolla, CA 92093-0085, USA
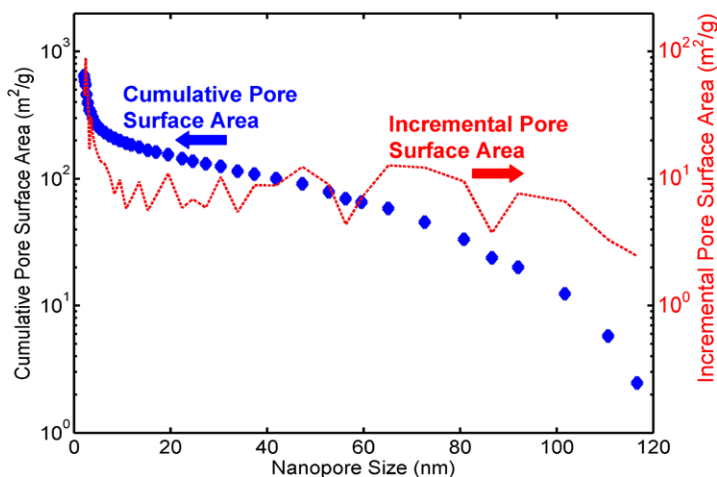e-mail: yqiao@ucsd.edu

T. Kim · Y. Qiao
Program of Materials Science & Engineering, University of California—San Diego, La Jolla, CA 92093, USA

X. Chen
Department of Earth & Environmental Engineering, Columbia University, New York, NY 10027, USA

The molecular structure of confined water is also highly dependent on the nanochannel size. When the channel size is relatively large, at the microscopic level, the layered molecular structure would vanish and the liquid properties can be described by the classic fluid mechanics [6]. If the nanochannel size is very small, close to the molecular size, the confined molecules would be forced into a quasi-one-dimensional chain, losing the characteristics of ordinary liquids [7]. When pressure increases, the effective density of the water molecular chain can increase, forming a double helical structure [8]. As temperature changes, the phase transform behavior of confined vapor, liquid, and solid-like phases is unique [9].

In an aqueous liquid, if there are solvated ions, many important properties would change significantly, such as the density, the critical conditions of phase transformation, and the viscosity [10]. Conventional fluid physics may be applied with the materials parameters being appropriately modified. In a nanochannel, especially when the nanochannel size is comparable with the ionic size, an electrolyte solution can no longer be regarded as a homogeneous material. The hydration shells would be distorted or even completely removed, so as to fit into the limited space [11]. The distorted hydration shell usually has a considerably higher free energy [12]. If the effective ion concentrations inside and outside nanochannel are different, the effective osmotic pressure must be balanced [13].

Recently, ionic liquids, which can be regarded as salt melts of relatively high melting points, have received increasing attention. Arguably, the best developed room-temperature ionic liquids that are stable in air and neutral are PF_6^- and BF_4^- compounds [14]. While they are toxic, these materials have found great applicability in a wide variety of areas, due to their low vapor pressures, wide working temperature ranges, excellent electrophysics and electrochemi-

Fig. 1 The nanopore size distribution

cal properties, etc. [15]. Very often, the cations are large and asymmetric, consisting of organic groups, e.g. 1-butyl-3-methylimidazolium (bmim). The anions are relatively small and inorganic, e.g. tetrafluoroborate (BF_4^-). The behavior of confined ions is critical to energy conversion, actuation, ion filtration, etc. [8–10]. The high ion mobility of the ionic liquid comes from the high melting point caused by the large cation size. The ion motion results in a high electric conductivity. It is expected that, when the ions in an ionic liquid approach a confining solid surface, particularly the inner surface of a nanochannel, nanotube, or nanopore, their behavior would be different from that of the solvated ions in an aqueous solution. First, the ions are not affected by the water molecule chain or layers. Second, without the hydration shells, the distortion or removal energy of water molecules is no longer relevant. Third, the ions are directly exposed to the solid atoms, significantly affecting the surface polarization. However, currently basic testing data of the effective interfacial tension and its dependence on nanopore size of confined ionic liquid are rare; this will be the focus of this study.

2 Experimental

We investigated 1-butyl-3-methylimidazolium tetrafluoroborate (bmimBF$_4$). The material was obtained from Sigma-Aldrich. At room temperature it was a viscous, clear liquid. Its molecular formula was $C_8H_{15}BF_4N_2$, with the molecular mass of 226. Its moisture content was less than 0.02 %.

The nanoenvironment was provided by using a nanoporous carbon, Cabot BP2000, which was in powder form and the particle size was about 50 μm. The nanoporous carbon was characterized by a Micromeritics ASAP-2000 Analyzer. The measured specific nanopore volume was 2.2 cm^3/g and the surface area was 1200 m^2/g. Figure 1 shows its pore size distribution. It can be seen that the pore

size distributed in a broad range from 2 nm to 100 nm. The average nanopore size was around 10 nm. The untreated carbon surfaces were decorated with charged sites such as hydroxyl groups, which can be strongly bonded with bmim cations. Thus, as the nanoporous carbon particles were immersed in bmimBF$_4$, they would be soaked up spontaneously without any external pressure, and during this process the information of system free energy change is relatively difficult to measure. In order to deactivate the polar surface groups, the carbon material was first dried in vacuum at 90 °C for 12 h, and then surface treated by chlorotrimethylsilane in dry toluene at 95 °C. The chlorotrimethylsilane content was 2.5 vol.%. The mixture of the carbon particles and the treatment reagents were refluxed for 48 h, after which the carbon was filtered and thorough washed by dry toluene and methanol. Finally, the treated carbon particles were dehydrated again in vacuum at 90 °C for 12 h.

At 20 MPa, 0.5 g of the treated carbon particles were compressed quasi-statically into disks, with the diameter of 19.2 mm. In a stainless steel cylinder, a carbon disk and 5.6 ml of bmimBF$_4$ were sealed by a stainless steel piston and the air bubbles were carefully removed. The piston was intruded into the cylinder at a constant rate of 1 mm/min, which induced a high inner pressure on the liquid phase. As the pressure was raised to about 14 MPa, the piston was moved out at the same speed to the original position. An external voltage, ϕ, was applied across the disk-liquid interface by a Proteck 6030 DC power supply. The carbon disk directly contacted the bottom of the stainless steel cylinder, which was connected to the cathode of the power supply. The anode was connected to a counter electrode immersed in the liquid phase through the upper piston. The counter electrode was a thin gold foil, separated from the carbon disk by a 100 μm thick porous polypropylene membrane. Due to the relatively high threshold voltage of bmimBF$_4$, the applied voltage could be as high as 3 V without any electrochemical
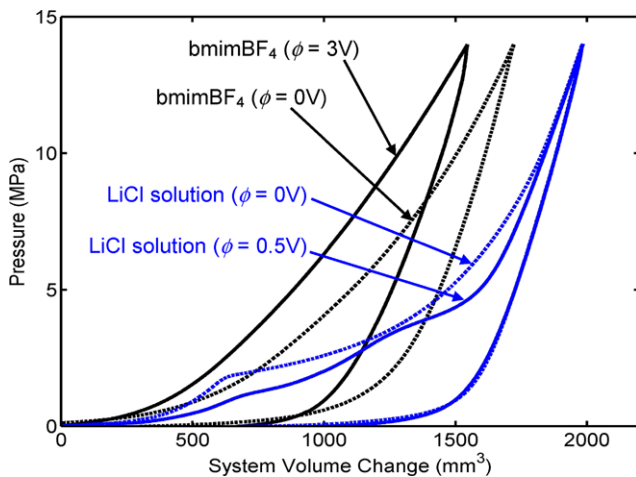
Fig. 2 Typical sorption isotherm curves with and without external electric field

surface reactions, while sufficiently low to avoid any morphology change of the nanopores. Typical sorption isotherm curves are shown in Fig. 2. Control tests were performed by using aqueous solution of electrolyte. The testing procedure was similar but the liquid phase was changed to 5.6 ml of saturated lithium chloride (LiCl) solution. The applied voltage was 0.5 V, below the threshold value to avoid electrochemical reactions.

3 Results and discussion

After the surface treatment, the carbon surfaces are covered by nonpolar silyl groups [16], and, thus, become nonwettable to both bmimBF$_4$ and LiCl solution. When the treated carbon particles are mixed with the liquid phase, the liquid cannot enter the nanopores unless a sufficient driving force is applied.

From Fig. 2, the pressure induced infiltration can be clearly seen. In the control test where there is no external electric field, i.e. when the applied voltage between the electrode and the counter electrode is zero, the sorption isotherm curve consists of a few stages. At the low-pressure stage, the system volume decreases slightly as the pressure rises, indicating that the compressibility of the electrolyte solution, the empty nanoporous particles, as well as the testing device is relatively low. When the pressure is increased to about 2 MPa, the slope of the curve abruptly decreases, suggesting that the liquid phase starts to be forced into the nanoporous space, leading to the rapid system volume reduction. Due to the pore size distribution, the infiltration process begins with the nanopores of a mild capillary effect, i.e. the relatively large nanopores, and smaller nanopores are filled up as the external pressure becomes higher. After the system is compressed by 1100 mm^3, the pressure rises to about 10 MPa

and the characteristics of infiltration vanish, indicating that the nanoporous space has been occupied. Further increasing pressure causes only a linear compression of the filled nanoporous particles and the surrounding liquid phase. The unloading path is quite different from the loading path; that is, the infiltration-defiltration process is highly hysteretic. The hysteresis may be related to the column resistance of nanopore walls, the confined gas/vapor phase, etc. [17–19], the reasons of which are still under investigation.

When an external electric field is applied, at a large solid surface, according to the conventional surface theory [20], the solid-liquid interfacial tension should decrease, following the classic Helmholtz–Perrin theory: $\gamma_{ls} = \gamma_{max} - \varepsilon_1 \varepsilon_0 \phi^2 / 2d_1$, with γ_{max} being the maximum interfacial energy, ε_1 the dielectric constant, ε_0 the permittivity of free space, and d_1 the characteristic length. This phenomenon can be observed in the nanoporous carbon in the control test: With the applied voltage, the infiltration of LiCl solution starts at only 1 MPa, 50 % lower than that of the previous case. That is, less external work is needed to overcome the repelling effect of the nanopore walls. If the effective interfacial tension, $\Delta\gamma$, can be assessed at the order-of-magnitude level by the Laplace–Young equation, $\Delta\gamma = P \cdot R / 2$, with P being the pressure and R being the effective nanopore radius, the decrease in $\Delta\gamma$ caused by the electric field is 25 mJ/m^2, which looks reasonable compared with the literature data [21]. In the above estimation, the effective nanopore size is taken as 50 nm.

The variation in $\Delta\gamma$ is quite nonuniform. As $\phi = 0.5$ V, there are two stages in the infiltration plateau. The low-pressure stage is between about 1 MPa and 2 MPa, and the high-pressure stage is from about 3 MPa to 4.5 MPa. Clearly, the $\Delta\gamma$–ϕ relationship is highly dependent on the nanopore size. When R is relatively large or relatively small, $\Delta\gamma$ rapidly decreases with the increasing of ϕ, corresponding to the low-pressure and high-pressure infiltration stages, respectively. When the nanoporous size is intermediate, $\Delta\gamma$ is relatively insensitive to the electric field. In a large nanopore, the solid-liquid interaction may be similar with that at a large surface; in a small nanopore, as the solvation structure is distorted and the ions are exposed to the nanopore inner surface at all directions, the effective coordination number of solid atoms interacting with a hydration shell increases, and, thus, the field effect can be amplified. In an intermediate nanopore, on the one hand, the nanopore inner surface can no longer be regarded as a large solid surface. The lack of the bulk phase suppresses the ion exchange along the radius direction, and, therefore, the degree of variation of ion structure is less pronounced, so is the effective infiltration pressure. On the other hand, the nanopore size is much larger than the ionic size, and the influence of the nanopore wall at the opposite direction is less important than that in a small nanopore. The combined effect of the two mechanisms results in the reduced sensitivity of $\Delta\gamma$ with respect to ϕ.

When the liquid phase is bmimBF$_4$, without the electric field, pressure induced infiltration can take place quite smoothly. However, the infiltration pattern is significantly different from that of the electrolyte solution. The infiltration starts almost immediately when the pressure is applied, indicating that in the largest nanopores the capillary effect is negligible. However, the involvement of smaller nanopores demands much higher pressures. At the highest pressure, the infiltration volume is only around 800 mm^3, about 25 % less than the infiltration volume of LiCl solution. The low pressure at the onset of infiltration shows that the effective interfacial tension between the carbon nanopore inner surface and bmimBF$_4$ is relatively low. The steep pressure increase in the infiltration plateau suggests that the nanopore wall has a pronounced repelling effect. Even when the nanopore surfaces are nominally wettable, there must be a "free volume" a few times larger than the ion [22, 23]. Because the bmim cations are relatively bulky, the required nanopore size is quite large. A high external pressure must be applied to "squeeze" the ions into a relatively small nanopore, causing the large slope in infiltration plateau. In the smallest nanopores, the infiltration cannot take place, and, consequently, the overall infiltration volume is reduced.

A remarkable phenomenon is observed when the electric field is applied across the carbon–bmimBF$_4$ interface: The infiltration pressure increases, contradictory to the prediction of the classic surface theory. As $\phi = 3$ V, the initial pressure at the onset of infiltration does not vary much, while the infiltration pressure in smaller nanopores increases considerably by 1–2 MPa. Even without the hydration shell, the effective solid–liquid interfacial tension should only decrease, since the surface charges in a solid surface always tend to repel the like-charged ions in the liquid phase. However, the repelling effect of the nanopore wall, particularly the requirement of the "free volume", can be of a different tendency. As the electric field is applied, the solid–ion interaction becomes much stronger, and the repelling effect is amplified. The increase in infiltration pressure may also be associated with the higher effective ion density caused by the applied voltage, so that the potential energy among adjacent cation–anion pairs increases, and the total energy barrier offered by the nanopore wall is higher. This effect also explains that the infiltration volume decreases with the application of the voltage, since the liquid infiltration in the smallest nanopores becomes more difficult.

4 Concluding remarks

To summarize, the behavior of electrolyte solution in the nanopores of a nanoporous carbon fits with the prediction of conventional surface theory, while there exists a significant nanopore size effect, which causes the nonuniform decrease in pressure across the infiltration pressure. The behavior of bmimBF$_4$, however, conflicts with the classic theory. As a voltage is applied, the required infiltration pressure increases and the infiltration volume decreases, suggesting that the liquid infiltration in the relatively small nanopores is more difficult. This unique phenomenon may be attributed to the direct interaction among the ions and the nanopore wall, promoted by the external electric field.

References

1. H. Daiguji, Ion transport in nanofluidic channels. Chem. Soc. Rev. **39**, 901–911 (2010)
2. P. Abgrall, N.T. Nguyen, *Nanofluidics* (Artech House, Norwood, 2009)
3. B. Xu, L. Liu, Q. Zhou, Y. Qiao, J. Xu, Y. Li, M. Tak, T. Park, X. Chen, Energy dissipation of nanoporous MFI zeolite under compressive loading. J. Comput. Theor. Nanosci. **8**, 881–886 (2011)
4. G.X. Cao, Y. Qiao, Q.L. Zhou, X. Chen, Water infiltration behaviors in carbon nanotubes under quasistatic and dynamic loading conditions. Mol. Simul. **34**, 1267–1274 (2008)
5. A. Holtzel, U. Tallarek, Ionic conductance of nanopores in microscale analysis systems: where microfluidics meets nanofluidics. J. Sep. Sci. **30**, 1398–1419 (2007)
6. L.D. Landau, E.M. Lifshitz, *Fluid Mechanics* (Butterworth-Heinemann, Oxford, 1987)
7. X. Chen, G. Cao, A. Han, V.K. Punyamurtula, L. Liu, P.J. Culligan, T. Kim, Y. Qiao, Nanoscale fluid transport: size and rate effects. Nano Lett. **8**, 2988–2992 (2008)
8. L. Liu, X. Chen, W. Lu, A. Han, Y. Qiao, Infiltration of electrolytes in molecular-sized nanopores. Phys. Rev. Lett. **102**, 184501 (2009)
9. B. Xu, Y. Qiao, M. Tak, T. Park, Q. Zhou, X. Chen, A conceptual thermal actuation system driven by interface tension of nanofluids. Energy Environ. Sci. **4**, 3632–3639 (2011)
10. B. Xu, Y. Qiao, Y. Li, Q. Zhou, X. Chen, An electroactuation system based on nanofluids. Appl. Phys. Lett. **98**, 221909 (2011)
11. R.B. Schoch, J.Y. Han, P. Renaud, Transport phenomena in nanofluidics. Rev. Mod. Phys. **80**, 839–883 (2008)
12. A.A. Milischuk, B.M. Ladanyi, Structure and dynamics of water confined in silica nanopores. J. Chem. Phys. **135**, 174709 (2011)
13. J. Zhao, P.J. Culligan, Y. Qiao, Q. Zhou, Y. Li, M. Tak, T. Park, X. Chen, Electrolyte solution transport in electropolar nanotubes. J. Phys. Condens. Matter **22**, 315301 (2010)
14. H. Ohno, *Electrochemical Aspects of Ionic Liquids* (Wiley, New York, 2011)
15. J. Mun, H. Sim, *Handbook of Ionic Liquids: Properties, Applications, and Hazards* (Nova Science Publishers, New York, 2011)
16. A. Han, Y. Qiao, Controlling infiltration pressure of a nanoporous silica gel via surface treatment. Chem. Lett. **36**, 882–883 (2007)
17. Y. Qiao, L. Liu, X. Chen, Pressurized liquid in nanopores: a modified Laplace–Young equation. Nano Lett. **9**, 984–988 (2009)
18. A. Han, X. Kong, Y. Qiao, Pressure induced infiltration in nanopores. J. Appl. Phys. **100**, 014308 (2006)
19. Y. Qiao, G. Cao, X. Chen, Effects of gas molecules on nanofluidic behaviors. J. Am. Chem. Soc. **129**, 2355–2359 (2007)
20. A.J. Bard, L.R. Faulkner, *Electrochemical Method: Fundamentals and Applications* (Wiley, New York, 2000)
21. J.O. Bockris, A.K.N. Reddy, M. Gamboa-Aldeco, *Modern Electrochemistry* (Kluwer Academic, New York, 1998)

22. A. Han, Y. Qiao, Pressure induced infiltration of aqueous solutions of multiple promoters in a nanoporous silica. J. Am. Chem. Soc. **128**, 10348–10349 (2006)

23. F.B. Surani, X. Kong, Y. Qiao, Two-staged sorption isotherm of a nanoporous energy absorption system. Appl. Phys. Lett. **87**, 251906 (2005)